TREATMENT OF DIFFRACTION EFFECTS CAUSED BY MOUNTAIN RIDGES

Rainer Klostius, Andreas Wieser, Fritz K. Brunner
Institute of Engineering Geodesy and Measurement Systems,
Graz University of Technology, Steyrergasse 30, A-8010 Graz, Austria.
E-mail: {rainer.klostius, andreas.wieser, fritz.brunner} @TUGraz.at

Abstract

A major problem of using GPS for deformation monitoring is signal distortion caused by the objects which form the skyline. Both local obstacles, like trees surrounding the station, and far away obstacles, like mountain ridges, lead to diffraction of the signal. In this paper we show data with corresponding biases in the observations up to 7 cm and a C/N_0 reduction of 10-12 dB.

We discuss three different approaches to mitigate such errors. First we discuss the usage of a constant high cut-off angle when collecting or processing the observations. Alternatively, we investigate the usage of an azimuth-dependent elevation mask to cut out the affected observations. In the third approach, we discuss the mitigation of the effect using different variance models.

The results show that a sufficiently high constant cut-off angle avoids diffraction effects at the obstacles, but the resulting bad geometry significantly reduces the attainable accuracy. The mitigation of the effects can either be reached by an appropriate azimuth-dependent elevation mask, or by using a variance model based on the signal-to-noise ratio, i.e. the SIGMA-ε variance model.

1. Introduction

In engineering geodesy, deformation measurement using GPS is a common technique, e.g. for the monitoring of landslides or buildings. Obstacles between the receiver and the satellite may degrade the signal quality and therefore the results. Often these obstacles affect mainly low elevation satellite data, but in an alpine environment, trees or mountain ridges may cause problems also at higher elevation angles. With static applications and long site occupation times, this may still not be a problem, because of the inherent long averaging time. For monitoring applications with kinematic processing or averaging over short times, the impact of diffraction may not be negligible.

The easiest way to eliminate a possible degradation of the signals is to use a sufficiently high elevation cut-off angle, higher than all obstructions. The observations possibly affected by the obstacles are then not used to compute the solution and thus cannot degrade the quality of the results. However, this approach may also reject many good observations, and it degrades the geometry of the solution. Instead, an optimum elevation mask could be derived from the physical horizon, possibly with a small offset. However, the application of such an azimuth-dependent elevation mask requires the horizon to be mapped in advance.

An alternative for mitigating the effect of such obstacles is to use variance models which reduce the impact of the distorted observations on the results. A standard approach for high precision applications is to work with an elevation dependent model, as it is e.g. implemented in the Bernese GPS-Software [1]. Another approach, the SIGMA-ε variance model developed by Hartinger and Brunner [2], uses the carrier-to-noise density ratio (C/N_0) as an input for computing the variances. Due to the antenna gain pattern, the C/N_0 value depends on the elevation of the arriving signal. However the C/N_0 also reflects actual signal distortions and is thus a more useful discriminator of the signal quality than the elevation alone.

In the next section we briefly review the effect which occurs, when satellites rise and set behind an obstruction. In section 3, the data set and the processing schemes used for the subsequent investigation are presented. Section 4 shows the diffraction effects in the observation and coordinate domain, and demonstrates the impact of selecting an appropriate elevation mask. The analysis also shows that using a proper variance model (SIGMA-ε) is another useful tool to suppress the deteriorating effect of the obstacles on the results, even if no specially matched azimuth-dependent elevation mask can be used.

2. Diffraction effects

When an obstacle interferes with the line-of-sight between the satellite and the receiver, one possible effect is the diffraction of the signals. The diffraction allows the GPS-signals to propagate beyond the horizon and behind obstructions. The received field strength in the receiver decreases rapidly as the satellite moves into a shaded region, but this diffracted field still exists, and has often sufficient strength to allow tracking by the receiver.

Diffraction effects can be explained by Huygen's principle. This principle states, that all points on a wavefront can be seen as point sources, which produce secondary wavelets. These wavelets create a new wavefront. Diffraction occurs when these secondary wavefronts propagate into the shaded region. Diffraction loss arises from the blockage of secondary waves, such that only a portion of the initially available energy is diffracted around an obstacle. Additionally, diffraction leads to an increase of the path length of the signal.

In order to roughly estimate the diffraction loss expected at mountain ridges, we assume that the mountain acts as a knife-edge with which the wavefronts interact, see Figure 1.

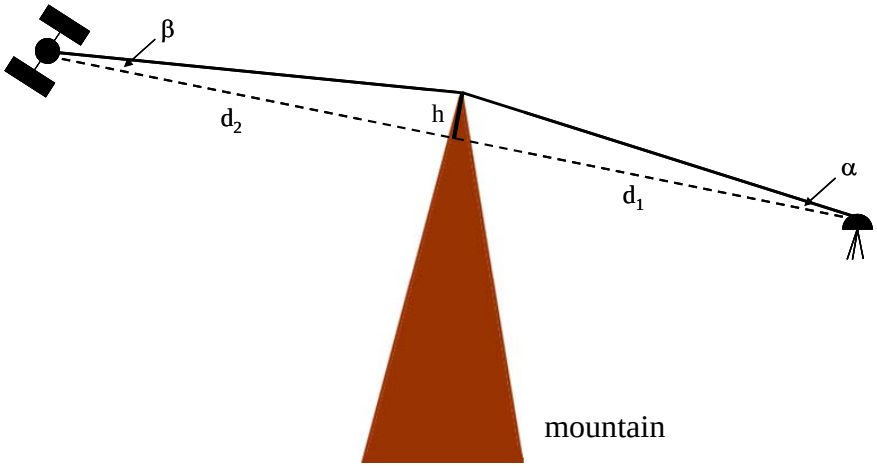

Figure 1: Geometrical representation of the knife-edge effect.

Using equation (17) in [3] and the geometric relations given in Figure 1, we can compute the diffraction loss of the signal. The result is visualized in Figure 2 (a) as a function of the angle α in Figure 1. Assuming a mountainous area, the obstructions occur at an elevation of 15-30°. The C/N_0 of the received signal in such elevations for the used equipment is in the unobstructed case in the range of 45-50 dBHz. In our case the used Ashtech receivers can not track signals lower than 35 dBHz, therefore signals can still be tracked until the loss of signal strength due to obstructions exceeds about 15 dBHz. From Figure 2 (a) follows that satellites will be tracked until they are, for example 0.3° below the mountain ridge in a distance d_1 of 5 km away from the receiver, which is a typical distance for the dataset chosen below.

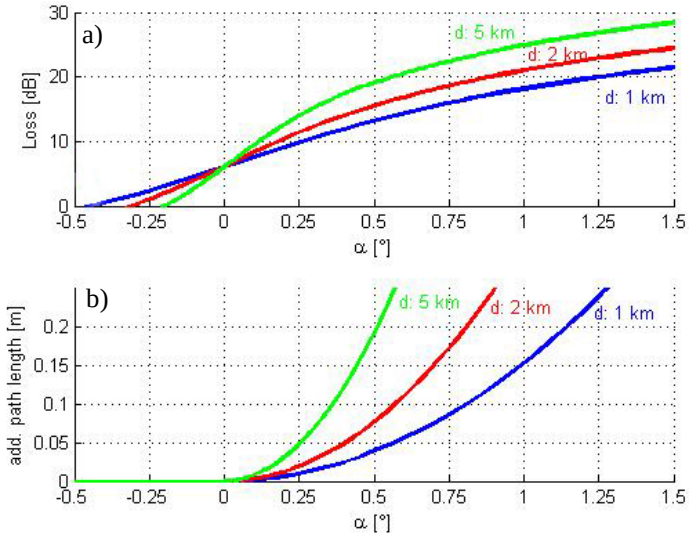

Figure 2: Diffraction loss (a) and additional path length (b) of the signal for distances of 1, 2 and 5 km from the receiver to the obstruction.

From Figure 1 we can also estimate the additional path length caused by diffraction. The result is shown in Figure 2 (b), again as a function of α. Using the above tracking threshold in terms of α (0.3°), we find that the maximum additional path length i.e., the maximum bias of the carrier-phase observable, due to diffraction by the mountain ridge will be approximately 70 mm.

3. Data processing

To visualize the diffraction effects and the possible consequences on the coordinate results, data of a GPS campaign are investigated. The campaign was measured at the Gradenbach landslide located in the northwest of Carinthia, cf. [4]. For this investigation, one 24 hour data set (Dec 12th 2005 12:00 UT to Dec 13th 2005 12:00 UT) for the baseline from reference point R2 to monitoring point MB, was chosen arbitrarily. Table 1 summarizes key parameters of this data set. The obstruction situation in terms of azimuth and elevation of the physical horizon on the two points was measured using a theodolite. Figure 3 gives an impression of the situation at both sites. The distribution of signal strengths (high C/N_0 at high elevation, low C/N_0 at low elevation) is mainly caused by the antenna gain pattern. We note that the mountain ridges cause a rather sharp cut-off of the GPS-signals. The trees do not cause such a sharp cut-off (see separate mask at MB). A detailed investigation also shows a difference between rising and setting satellites. The signal acquisition threshold is usually higher than the signal tracking threshold in a receiver, meaning that the signals have to be stronger for acquisition. Consequently, satellites may be first tracked at higher elevations than when they

set. Due to a lack of time only the combined obstruction mask was obtained at the station R2. The following investigation thus concentrates on signals which are affected by the obstructions at MB, because of the possibility to distinguish between trees and mountain, there.

Table 1: Outline of Gradenbach data sets chosen for this investigation; scale parameters used subsequently with identical-variance model (ID), elevation dependent variance model (ELE), and SIGMA-ε variance model (EPS); coordinate random walk spectral noise density (Q) for each of North, East, and Height.

Reference	Antenna	Ashtech Chokering
	Receiver	Ashtech Z-Xtreme
Rover	Antenna	Ashtech Chokering
	Receiver	Ashtech Z-Xtreme
Sampling rate [s]		3
Elevation cut-off angle [°]		0
Baseline length [km]		3.2
ID: σ [mm]		5.6
ELE: σ_0 [mm]		1.4
EPS: C [m^2Hz]		1.21
Q [m²Hz]		0.01

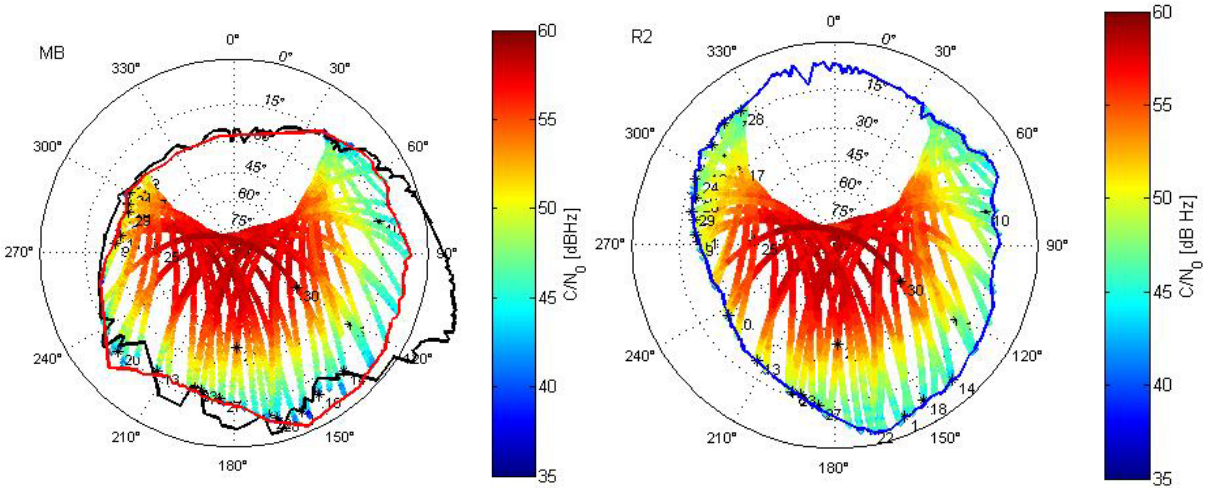

Figure 3: Satellite tracks with measured C/N_0 values at stations MB (left) and R2 (right); obstruction masks on MB: mountains (red), trees (black); combined obstruction mask on R2 (blue).

For this data set, the investigation of the effects in the observation domain was carried out using double-differenced (DD) 'observed-minus-computed' (OC) values:

$$OC = \nabla\Delta\Phi - (\nabla\Delta\rho + \nabla\Delta I + \nabla\Delta T + \nabla\Delta\delta^s \cdot c + \nabla\Delta PCV + \nabla\Delta N) \quad (1)$$

$\nabla\Delta\Phi$ … DD observed phase (m)
$\nabla\Delta\rho$ … DD geometrical range, incl. antenna offset and relativistic corrections (m)
$\nabla\Delta T$ … DD tropospheric correction (m)
$\nabla\Delta I$ … DD ionospheric correction (m)
$\nabla\Delta\delta^s$ … DD satellite clock error (s)
c … speed of light in vacuum (m/s)
$\nabla\Delta PCV$ … DD phase centre variations (m)
$\nabla\Delta N$ … DD initial carrier-phase ambiguity

The OC values were computed using a Kalman Filter MATLAB-package developed at the Institute of Engineering Geodesy and Measurement Systems. As input parameters precise IGS orbits, the Saastamoinen tropospheric model and the Klobuchar ionospheric model were used. The phase centre eccentricities and variations of the used antennas were taken into account using the NGS antenna calibration results which are available on the internet[1]. The station coordinates were assumed constant during the 24 hour session, and were taken from previous static processing of the same data using the Bernese GPS-software. Due to the short baseline length in this campaign (see Table 1), we may assume that most of the effects due to ionosphere and troposphere are eliminated by double-differencing and application of the above models. Furthermore, we know that there was no significant motion during the selected session time, so the patterns found subsequently in the OC time series and the coordinate time series are caused by noise and propagation effects like diffraction and multipath.

For the analysis in the coordinate domain, the coordinates of the respective reference point were fixed and those of the rover point were estimated as coordinate random walk using the Kalman Filter program of the above mentioned MATLAB-package. The spectral noise density Q (see Table 1) was deliberately set much higher than the expected motion of the points would require. This allows the estimated coordinates to vary as indicated by the observations and thus show the real impact of distorted observations. It has to be mentioned, that a quality control kernel which performs outlier detection and mitigation is an integral part of the Kalman Filter package and was used during calculation of the coordinate time series.

For the analysis of the effects in the observation domain, OC values computed by the same Kalman Filter program were used (because the ambiguities have to be fixed), but the coordinates of the rover stations were constrained to their initial (true) values. So the OC values represent the error patterns except during periods (few epochs only) with float ambiguities, which may absorb parts of the pattern.

Three different variance models were used: a variance model assuming identical variance of all observations (ID), an elevation dependent model (ELE), and the SIGMA-ε variance model (EPS) [2]. The ELE yields variances

$$\sigma^2_{ELE} = \frac{\sigma_0^2}{\sin^2(\varepsilon)}, \quad (2)$$

[1] http://www.ngs.noaa.gov/ANTCAL/

where ε is the elevation angle of the respective (undifferenced) observation, and σ_0 is given in Table 1. The formula for the EPS model is obtained by

$$\sigma^2_{EPS} = C \cdot 10^{\frac{-C/N_0}{10}}, \qquad (3)$$

where the computed variance of the individual undifferenced observations is a function of the measured C/N_0 value and a constant C (see Table 1), dependent on the GPS equipment used. The variances of the double differences are then obtained by variance propagation where the mathematical correlation is properly taken into account, but the undifferenced observations are assumed uncorrelated.

4. Results

Figure 4 shows a typical diffraction effect associated with a satellite setting behind the mountain. The top subplot contains the elevations of the satellite PRN18 (red) and of the reference satellite PRN29 (blue) for a time window of half an hour. The middle subplot shows the measured C/N_0 values of both satellites at the rover station MB, and the bottom subplot shows the time series of OC values. The C/N_0 values of PRN18 drop by about 12 dBHz within about 3 minutes, and the OC values show a related increase of 7 cm until the satellite finally sets. The Kalman Filter program used here was based on virtually fixed rover station coordinates. So it detects that there is a discrepancy and sets up a new float ambiguity for the double difference during this period. This causes the OC values to drop back to about 0 for some time. The discrepancy is not easily detectable if the rover station coordinates are actually estimated, see below.

Satellite PRN18 sets behind a mountain which is about 5 km away from station MB. The distance between the obstruction and the station was obtained roughly from a topographical map. According to Figure 2 (a), a drop of 12 dBHz due to a knife-edge obstruction 5 km away from the station (green line), is expected once the satellite sets 0.18° below the mountain skyline. From Figure 2 (b) we see that the additional path length at $\alpha = 0.18°$ is about 3 cm. In fact, the OC time series indicates an increase in path length of 7 cm, and the satellite sets 0.35° below the measured physical horizon. The observed effect agrees well with the simple model, despite the fact that the knife-edge model provides a rough estimation of the actual diffraction effect.

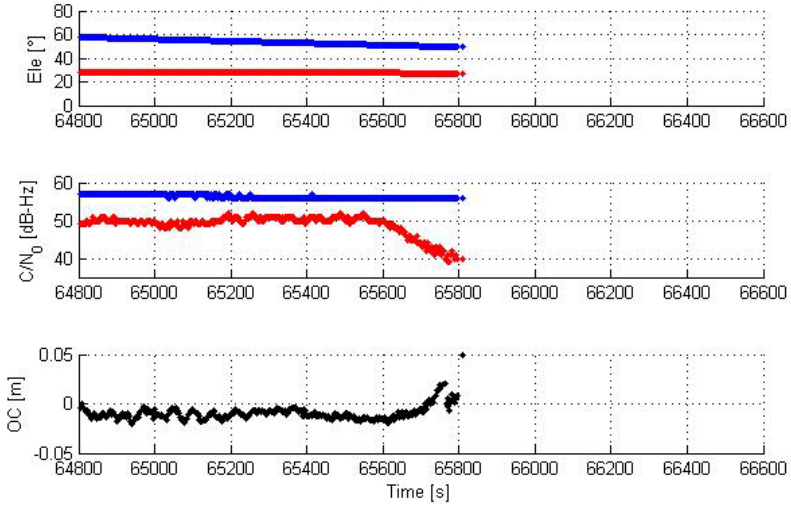

Figure 4: Elevation, C/N_0 (site MB), and OC for satellites PRN18 (red) and PRN29 (blue).

This diffraction effect can also be seen clearly in the time series of the estimated coordinates (Figure 5). Using a constant elevation cut-off of 15° (or lower), the observations of PRN18 contribute to the solution and cause coordinate errors of up to 2 cm horizontally and 7 cm vertically (blue). Using an elevation cut-off of 30° (magenta), all obstructions by mountains are lower than the elevation cut-off and will thus not cause any effects in the estimated coordinate time series. Actually, Figure 5 shows that using such a cut-off, the diffraction effect of PRN18 does not show up any more.

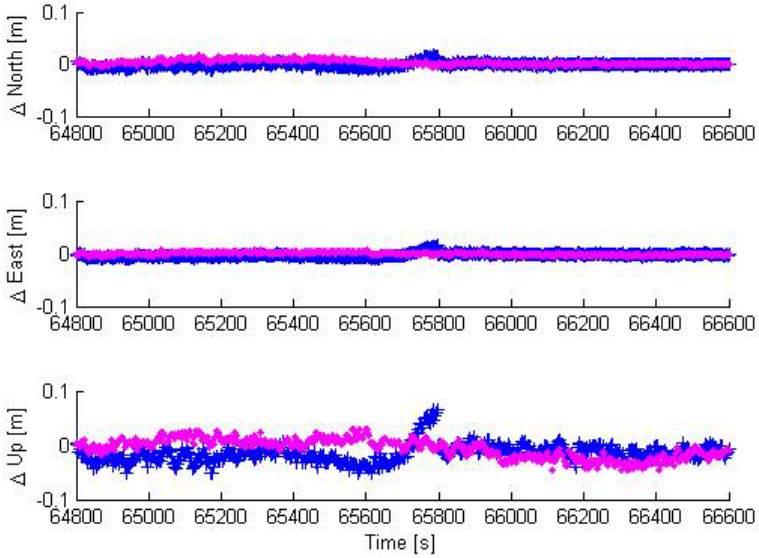

Figure 5: Deviation of estimated coordinate time series from ground truth during period with PRN18 setting behind a mountain; variance model: ID; 15° elevation cut-off (blue), 30° elevation cut-off (magenta).

However, using a 30° cut-off, 30% of the observations recorded by the receiver are discarded, and the geometry is deteriorated significantly. A scatterplot of the horizontal coordinates (Figure 6) calculated for the whole session confirms that a cut-off of 30° produces very poor results (Figure 6 (a)): the maximum coordinate error is about 1 m, and 20% of the position errors are outliers in the sense that they exceed 3σ (calculated as a robust empirical standard deviation). Even a constant cut-off angle of 15° causes a clear deterioration of the accuracy of the estimated positions (Figure 6 (b)) as compared to the constant cut-off of 5° (Figure 6 (c)). It can be shown that using the azimuth-dependent elevation mask, the diffracted observations of satellites shaded by the mountain ridge are not part of the solution any more. Figure 8 suggests that the subplots (c) and (d) both produce the same result. This is not true, but the differences mainly occur during the few and brief periods where a satellite is tracked while the line-of-sight is already (or still) obstructed by the mountains. These differences are hardly visible in the 24 hour scatter plots.

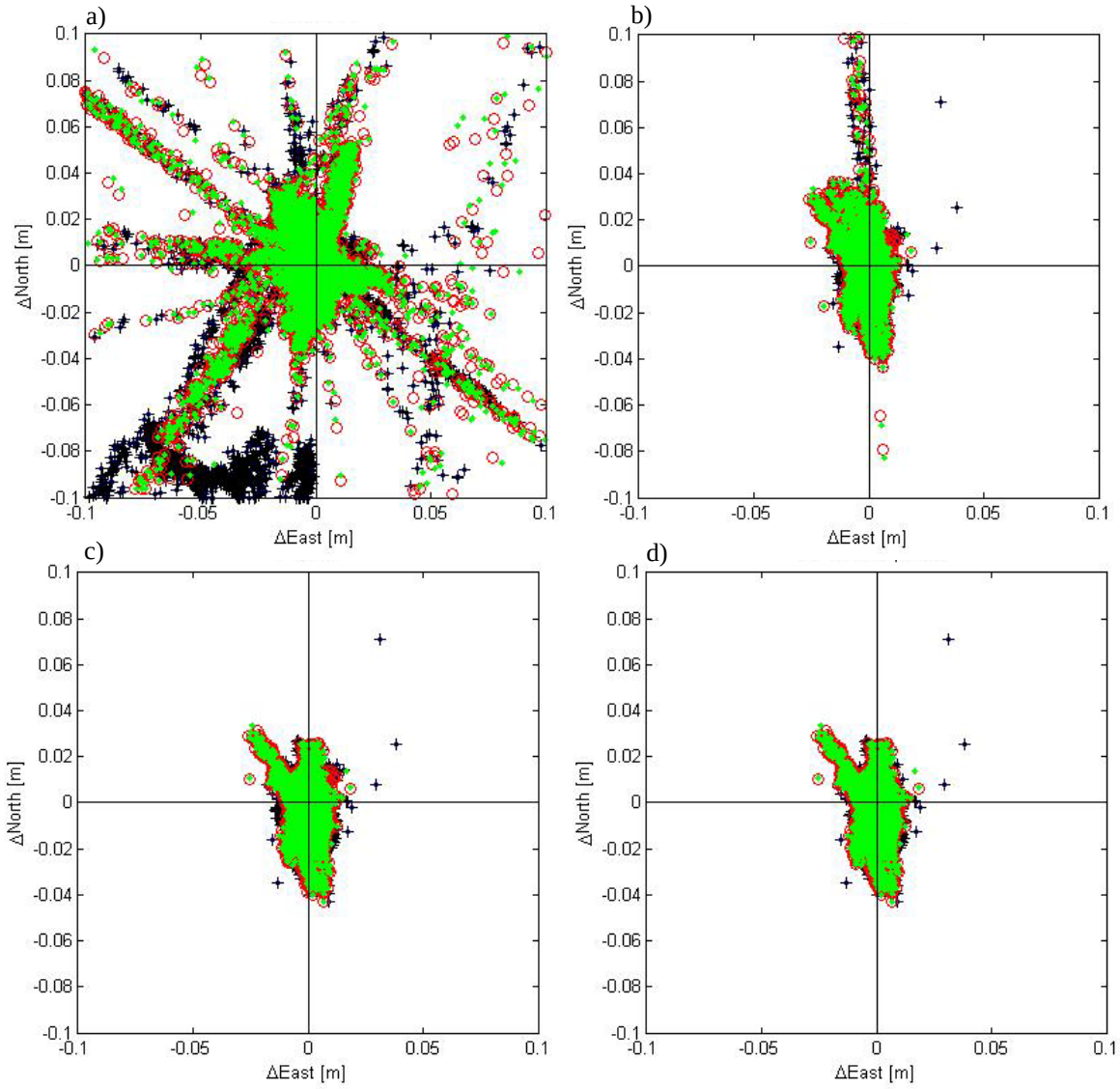

Figure 6: Deviations in North and East from the reference solution for the three variance models and different elevation masks (a) 30° cut-off, b) 15° cut-off, c) 5° cut-off, d) azimuth dependent cut-off), ID: +, ELE: o, EPS: •.

An alternative to measuring the azimuth and elevation of the physical horizon and using it as an azimuth-dependent elevation mask, is to employ a variance model which detects diffracted observations and mitigates their influence on the estimated coordinates. The effect of the three different variance models introduced in section 3 can be seen in Figure 7 for the same time window as before (with PRN18 setting behind the mountain). Note, that now the horizontal coordinates are plotted with a different scale than the deviation in the Height coordinate (Up). The carrier-phase observations were now processed using a 5° cut-off, so most of the diffracted observations were part of the data used to compute the coordinates. It can be seen, that the EPS model (green) largely mitigates the diffraction effect, whereas the ELE model (red) and the ID variance model (black) do not.

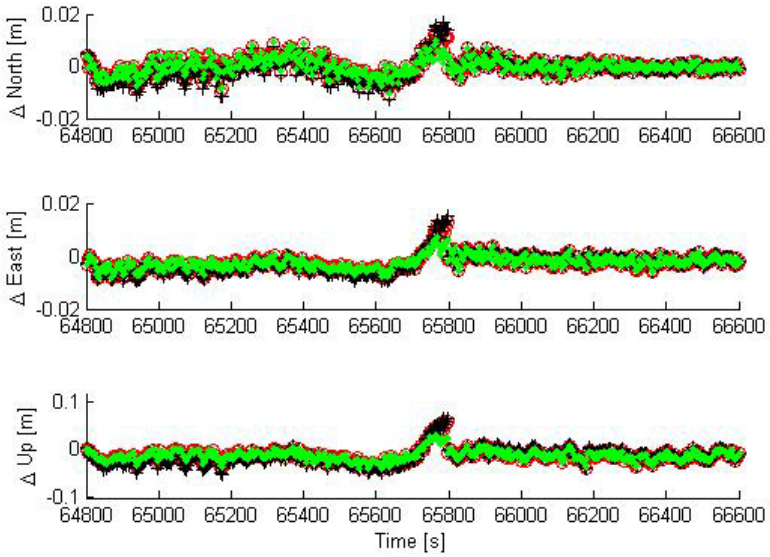

Figure 7: Deviation of the estimated North, East, Up coordinates from the reference solution for a 30 min time window (5° cut-off); ID: +, ELE: o, EPS: •.

Table 2 shows the standard deviation and the maximum values for the three coordinate time series plotted in Figure 7. It can be seen, that the EPS model has the lowest standard deviation and the smallest maximum errors. Reducing the length of the time window further cause an improvement by the EPS variance model to stand out even more. This confirms that the effect is more serious if kinematic coordinate results are needed, or if the coordinates are averaged over short periods only (short static solutions).

Each of the scatter plots in Figure 6 contains the results corresponding to all three variance models. We will not analyze the differences in detail, here. However, the plots confirm that the SIGMA-ε variance model gives generally higher accuracy than the elevation dependent variance model, and both perform significantly better than the ID variance model.

Table 2: Standard deviation (σ) and maximum absolute value of North, East, Up coordinate error w.r.t. ground truth for 5° elevation cut-off, and three different variance models (ID, ELE, EPS) for the 30 min time window as visualized in Figure 5.

Value	ID			ELE			EPS		
	N	E	U	N	E	U	N	E	U
σ [mm]	4	3	17	3	3	14	3	2	10
max [mm]	17	15	65	14	13	59	10	8	40

5. Conclusions

Using standard equations for the assessment of diffraction loss, we have shown that geodetic GPS receivers are expected to track satellite signals even when the satellites are slightly below the physical horizon. This causes a significant decrease in signal strength and an observation bias (diffraction error).

We have then shown experimentally that these effects are clearly visible in the 'observed-minus-computed' time series and in the measured C/N_0 values. Using data from an experiment in an alpine environment, we showed observation biases of up to 7 cm and

simultaneous attenuation (C/N_0 reduction) of 10–12 dB. We have also observed the effects in the data of other campaigns, which showed the same patterns in the C/N_0 and OC time series.

The processing results confirmed centimetre-level errors of the kinematically estimated coordinates if the diffraction effects are not taken into account. Using a high constant elevation cut-off angle the geometry may be deteriorated to a degree where the solution becomes useless for monitoring applications. Also, the use of an elevation dependent variance model cannot solve the problem. We have shown, that the diffraction effects can be eliminated by using an appropriate azimuth-dependent elevation mask, because the diffracted observations are then not part of the solution any more. The effect can also be mitigated using the SIGMA-ε model, due to the fact that the C/N_0 values reflect the diffraction effect.

Acknowledgments

This investigation was partially funded by the Austrian Academy of Sciences in the framework of the ISDR project 21/2005. R. Lummerstorfer and R. Neumayr helped with the Gradenbach experiment.

References

[1] Hugentobler, U., Dach, R., Fridez, P.: BERNESE GPS Software Version 5.0. Astronomical Institute University of Berne, 2004.

[2] Hartinger, H., Brunner, FK.: Variances of GPS Phase Observations: The Sigma-ε model. GPS Solutions 2/4:35-43, 1999.

[3] ITU: Propagation by diffraction. International Telecommunication Union, Recommandation, ITU-R P.526-6, 1999.

[4] Brunner, FK., Zobl, F., Gassner, G.: On the Capability of GPS for Landslide Monitoring. Felsbau 21(2):51-54, 2003.